

Experimental studies on the fatigue life of shape memory alloy bars

Sara Casciati*

Department ASTRA, University of Catania, Via delle Maestranze 99, 96100 Siracusa, Italy

Alessandro Marzi

Department of Structural Mechanics, University of Pavia, Via Ferrata 1, 27100 Pavia, Italy

(Received May 14, 2009, Accepted July 11, 2009)

Abstract. The potential offered by the thermo-mechanical properties of shape memory alloys (SMA) in structural engineering applications has been the topic of many research studies during the last two decades. The main issues concern the long-term predictability of the material behaviour and the fatigue lifetime of the macro structural elements (as different from the one of wire segments). The laboratory tests reported in this paper are carried out on bar specimens and they were planned in order to pursue two objectives. First, the creep phenomenon is investigated for two different alloys, a classical Ni-Ti alloy and a Cu-based alloy. The attention is then focused on the Cu-based alloy only and its fatigue characteristics at given temperatures are investigated. Stress and thermal cycles are alternated to detect any path dependency.

Keywords: creep; fatigue; hysteresis; shape memory alloys; thermo-mechanics; viscosity.

1. Introduction

In a special issue recently published in the Journal of “Smart Structures and Systems”, three papers, (Casciati and van der Eijk 2008, Olsen, *et al.* 2008, Casciati and Hamdaoui 2008), are dedicated to investigate the potential of deploying pre-tensioned shape memory alloys (SMA) wires/bars in the retrofitting of historical buildings, as it had already been proposed in references (Casciati and Faravelli 2008, Casciati and Osman 2005). Both an alloy having copper (Cu) as main component and a classical nickel-titanium (Ni-Ti) alloy were studied. Their thermo-mechanical response was investigated by an experimental campaign whose main results are summarized in this paper. Particular attention is devoted to detect the possible presence of dangerous viscous features. Indeed, when dealing with shape memory alloys, the retrofit designer cannot ignore the evolution of the material behaviour during its operational lifetime (Casciati and Faravelli 2004). Namely, one has to account for the thermal effects, the phase transformations, and the stabilizations (Otsuka and Wayman 1999, Montecinos, *et al.* 2006). Some constitutive models which include these aspects are available in literature, but their use is mainly effective at a micro-scale level (Auricchio, *et al.* 2001). A detailed overview of SMA applications in the

*Corresponding Author, E-mail: saracasciati@msn.com

field of civil engineering is provided in Casciati and Faravelli (2009). In all the studies, the SMA components are required to undergo loading-unloading cycles, thus demanding for preliminary fatigue tests to be carried out. Therefore, the experimental studies reported in this paper are targeted to the assessment of the fatigue lifetime of the Cu-based alloy, and to its potential improvement by performing a proper ageing and an adequate mechanical training.

2. Thermo-mechanical features of different alloys

The Cu-based alloy utilized for the tests reported in this paper is the same material, of label AH140, whose thermo-mechanical properties were investigated in (Casciati and van der Eijk 2008, Casciati and Faravelli 2004, 2006, 2009, Casciati, *et al.* 2007). The results of the differential scanner calorimeter (DSC) tests on the studied alloy, as well as on the Ni-Ti alloy AF5b introduced later, are reported in Table 1. For the purposes of this paper, a single cylindrical specimen of diameter 3.5 mm, which preliminarily underwent a thermal treatment consisting of heating at 850 °C for 10 min, followed by cooling at ambient temperature, and finally re-heating at 100 °C for 2 h, is tested in tension and its strain is measured by an extensometer. The test is conducted in span control during the loading, and in load control during the unloading. Ten cycles at ambient temperature up to the strain of 2% are applied in order to perform the so-called “mechanical training”. They are followed by four series of three cycles each, again up to the maximum strain of 2%, at the temperatures of 30 °C, 60 °C, 90 °C, and 120 °C, respectively. The test speed is 0.005 mm/s. Fig. 1 summarizes the test results in terms of the stress-strain relationships obtained at different temperatures. The main features emphasized by these diagrams confirm what is commonly reported in the literature: the “knee” stress and the residual strain increase as the temperature increases, while the width of the hysteric loop decreases.

Table 1 Results from the DSC tests on the two different alloys investigated in this paper

	M_f	M_p	M_s	A_s	A_p	A_f
AF5b	-48 °C	-41 °C	-29 °C	8 °C	14 °C	17 °C
AH140 treated	-38 °C	-29 °C	-20 °C	-17 °C	-12 °C	0 °C

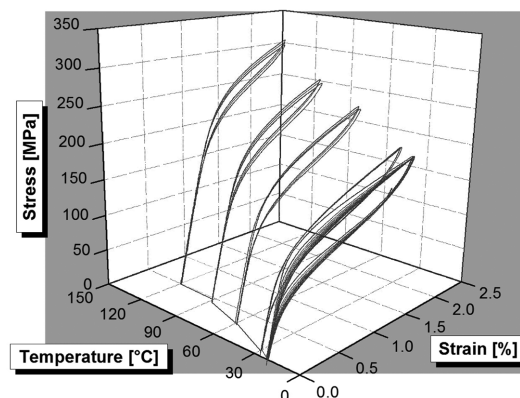


Fig. 1 Cyclic tension test up to a strain of 2% on the Cu-based alloy AH140 after applying a suitable thermal treatment (heating at 850 °C for 10 minutes, cooling at ambient temperature and re-heating at 100 °C for 2 hours)

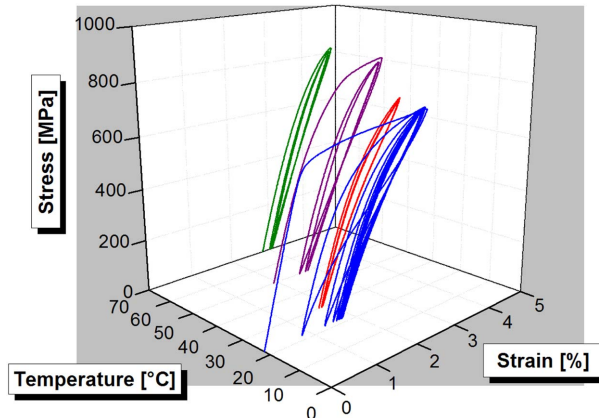


Fig. 2 Cyclic tension test up to a strain of 4% at ambient temperature and at 30 °C, and up to 5% strain at 50 °C and at 70 °C, on the Ni-Ti alloy AF5 (as acquired from the manufacturer)

The second tested material is a 5.3 mm cylindrical specimen of the AF5 Ni-Ti alloy described in (Olsen, *et al.* 2008). Being this alloy more ductile than the Cu-based one, a deformation limit of 4% was adopted for the cycles at ambient temperature and at 30 °C, and it was then increased to 5% for the further two tests at 50 °C and 70 °C, respectively. The results of these tests are plotted in Fig. 2. The same features observed in Fig. 1 are also present in Fig. 2. However, there is an abnormal residual displacement at the end of the cycles performed at ambient temperature. Its value is so significant that the subsequent tests at higher temperatures, up to a strain level of 5%, are unable to reach the relevant “knee” stress. To verify the results of Fig. 2, further tests were conducted on the Ni-Ti bars (Casciati and Faravelli 2009, Casciati and Marzi 2008), which are summarized as follows:

- (a) a tension branch in strain control up to 2% of deformation is followed by a branch in load control, during which the load is maintained constant for 10 min. The unloading is then performed in load control. As shown in Fig. 3(a), the bar undergoes an unexpected deformation under constant load (up to more than 4%) and, after the unloading, a residual deformation of 1.1% is observed;
- (b) a tension branch in strain control up to 2% of deformation is followed by a branch in load control, during which the load is maintained constant for 10 min and the temperature is increased up to 60 °C at the rate of 0.2 °C/sec. Always in constant load control, the temperature is then decreased, at the same rate, until it reaches 30 °C. The sample is left for 1 hour at this temperature. As Fig. 3(b) shows, the bar once again undergoes the unexpected deformation under constant load (up to more than 4%). The warming and cooling steps only enable a full recovery of the further elongation.
- (c) a test similar to the previous one consists of reaching a deformation of 4% in strain control, increasing the temperature up to 60 °C at the rate of 0.1 °C/sec while maintaining the load constant for 30 min, and performing the final unloading. Fig. 3(c) shows the corresponding stress-strain-temperature diagram.

From the results, it can be observed that the Cu-based alloy presents the main advantage of avoiding undesirable creep phenomena. This capability is mainly achieved by preliminarily performing a suitable thermal treatment and it could be improved by applying an adequate mechanical training. These two aspects will be further developed later in the text. Although the Cu-based alloy offers less

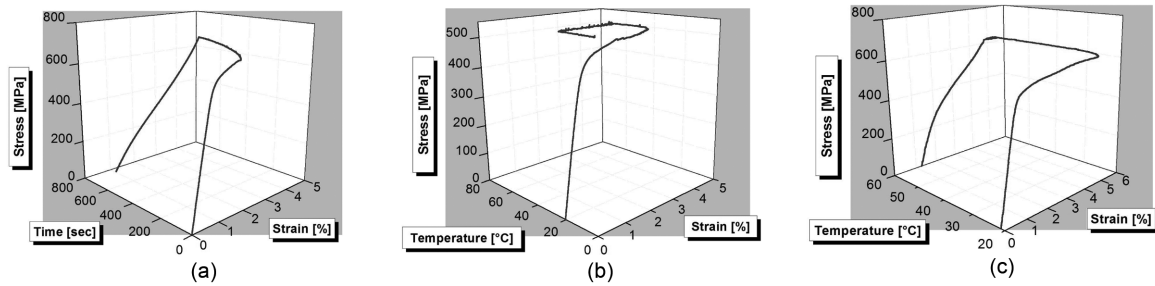


Fig. 3 Stress-strain diagram for the AF5 Ni-Ti alloy: (a) after reaching a strain of 2%, the load is maintained constant for 10 min and then the unloading is performed; (b) once reached a strain level of 2%, the load is maintained constant for 10 min. and the temperature is increased up to 60 °C; after a fast cooling to 30 °C, the specimen is left at this temperature for 1 hour; (c) once reached a strain level of 4%, the load is maintained constant for 30 min. and the temperature is increased up to 60 °C, then the final unloading is performed.

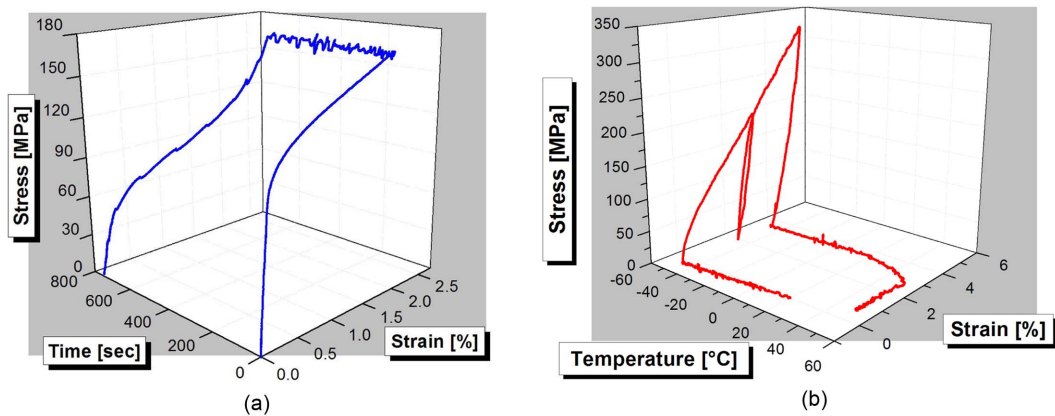


Fig. 4 Stress-strain diagram for the AH140 Cu-based alloy: (a) after reaching a strain level of 2%, the load is maintained constant for 10 min., and then a final unloading is performed; (b) test conducted at -50 °C with final heating to the ambient temperature.

deformation capability than the Ni-Ti alloy, it is also less expensive and shows a broader temperature window in which the austenite hysteresis occurs (see Table 1).

A further test at -50°C is performed on the Cu-based alloy to investigate its behaviour in martensite phase. The specimen, initially at ambient temperature, is cooled down to -50 °C and it is left at this temperature for 10 min. The loading then is performed in span control up to a deformation of 3%. After the unloading, another loading is performed causing a further increase of 3% of the strain. At the end of the final unloading, a significant amount of residual strain is observable. To recover the residual strain, the specimen, suddenly exposed to ambient temperature, is slowly heated up to 50 °C and then it is left at this temperature for 6 min.

The martensite phase is characterized by a significant hardening as observable from the steep loops of shown in Fig. 4(b). This feature is observed also in the shape of the deteriorated cycles resulting from the fatigue tests discussed in the next sections.

3. Fatigue performance of the copper-based alloy

The adoption of SMA structural elements in any civil engineering application requires that the material has a fatigue lifetime of at least 1000 working cycles (Torra, *et al.* 2007, Casciati, *et al.* 2008). A maintenance policy which guarantees a periodic replacement of such elements should be envisioned in their design. Other applicability requirements are that pauses between sets of cycles should not induce changes in the hysteresis, and that the SMA devices should be able to work in summer and winter without showing any parasitic phenomena (Torra, *et al.* 2009). The study of the thermo-mechanical properties of the Cu-Al-Be SMA discussed in the previous section suggests that an appropriate behaviour can be potentially maintained during a sufficient number of fatigue cycles, provided that the specimen preliminarily underwent a thermal treatment of 10 min at 850 °C and of 2 hours at 100 °C. To further investigate this aspect, the progressive evolution of the fatigue life is studied at two different temperatures; namely, at 30 °C and at 50 °C. At each temperature, four tests have been performed in span control by fixing different upper limits of the displacement, whose lower limit is always assumed equal to 0.35 mm, in order to avoid negative values of the stress during the unloading. The details of each test in span control are given in Table 2. To validate the results, two further tests at 50 °C have been performed in load control. They are represented by the triangular data points in Fig. 5, and they consist of 15537 cycles up to a maximum stress of 207 MPa, and of 1611 cycles up to a maximum stress of 253 MPa, respectively. This maximum stress values correspond to initial maximum strains of 3.5% and 1.6% respectively.

In Fig. 5(a) and 5(b), the total number of cycles obtained from each test is plotted versus the associated maximum stress and maximum strain, respectively. When the specimen is operated at a high temperature (50 °C), a reduced fatigue lifetime is recorded with respect to the performance obtained at nearly ambient temperature (30 °C). In Fig. 5(b), the results obtained from both the tests at 30 °C and 50 °C show a regular trend which can be easily interpolated by an exponential curve. Instead, the points collected in Fig. 5(a) follow an S-shaped curve whose slope increases with the temperature. By inspecting the points in Fig. 5(b), the flex can be located at a strain of 3.5%.

The results in terms of maximum stress, σ_{\max} , versus number of cycles obtained from the pair of tests at 50 °C in load control are consistent with the ones obtained from the tests in span control at the same temperature, since the triangular data points in Fig. 5(a) can be interpolated by the same S-shaped curve used to interpolate the other points. Instead, a discrepancy is observed when the results are plotted in terms of maximum strain, ϵ_{\max} , versus the number of cycles (Fig. 5(b)). This apparent discrepancy

Table 2 Results of the fatigue tests in span control

Temperature [°C]	Max span [mm]	Min span [mm]	Strain upper bound [%]	Strain lower bound [%]	Number of cycles
30	0.641	0.351	2.10	1.16	156500
	0.787	0.351	2.60	1.16	32800
	0.877	0.351	2.90	1.16	15826
	1.22	0.351	4.00	1.16	3271
50	0.64	0.351	2.10	1.16	73247
	0.787	0.351	2.60	1.16	19602
	0.876	0.351	2.90	1.16	13032
	1.224	0.351	4.00	1.16	2078

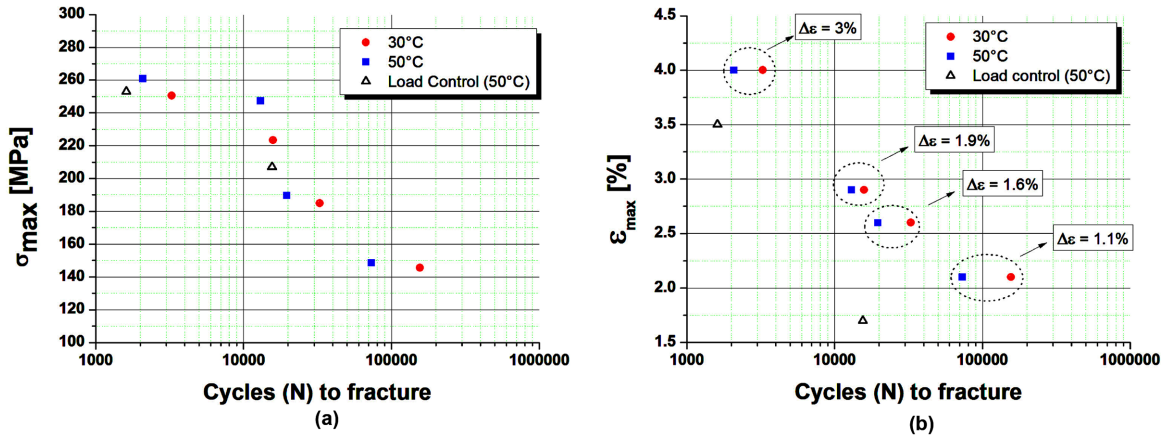


Fig. 5 Fatigue tests on a CuAlBe bar of 3.5 mm diameter: (a) number of cycles vs. maximum stress; (b) number of cycles vs. maximum strain. The cycling is performed at 1 Hz and at two different temperatures: 30 °C and 50 °C. All tests are performed in span control, except for the two triangular points obtained in load control at 50 °C.

would not be present if the ordinates of the graph in Fig. 5(b) were expressed in terms of the strain range, $\Delta\epsilon$, since in this case the curves obtained in span control would shift downward of an amount equal to the fixed minimum strain, $\epsilon_{min} = 1.16\%$. However, in the more general case in which the minimum strain varies from a test to another, the representation of the strain range alone is not sufficient, and also the values of the maximum strain must be provided in order to have a full description of the test results. Therefore, both parameters are specified in the plot of Fig. 5(b). To further investigate the discrepancy of the maximum strain values obtained from the tests in load control with respect to the ones assigned in span control, Fig. 6 shows their time evolution during each test in load control, together with the time evolution of the minimum strain. A third curve obtained as the difference between the other two curves is shown in each plot of Fig. 6 to represent the time evolution

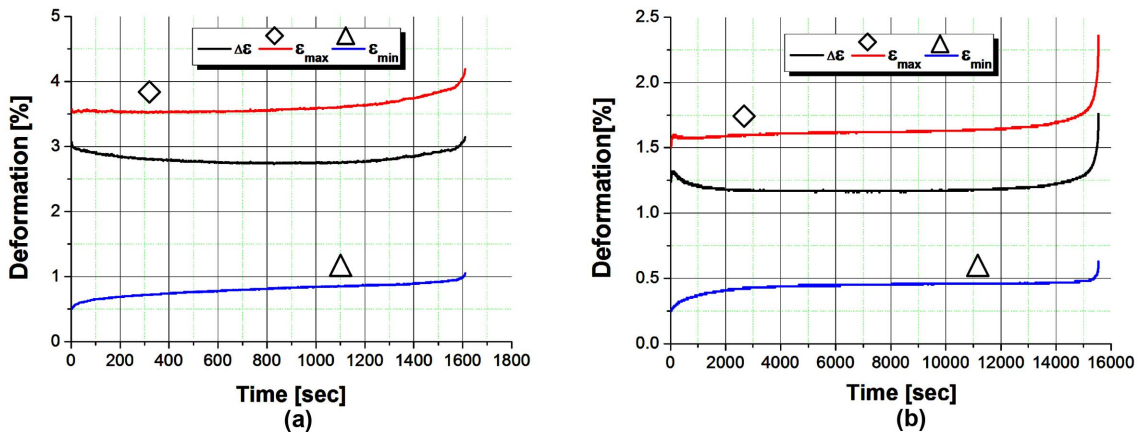


Fig. 6 Fatigue tests on a CuAlBe bar of 3.5 mm diameter driven in load control: evolution of strain range and of the minimum and maximum value of the deformation: (a) maximum stress of 253 MPa (maximum initial strain of 3.5%); (b) maximum stress of 207 MPa (maximum initial strain of 1.6%).

of the strain range, $\Delta\varepsilon$, during each test. Theoretically, the maximum strain should coincide with the strain range at the beginning of the test, since the minimum strain should be null. However, from Fig. 6 it is evident that the actual non return to zero after the first unloading and the progressive material deterioration due to the creep phenomenon cause an increase of the minimum strain and a consequent decrease of the strain range. At one half of the test duration, a further phenomenon occurs: a progressively higher maximum strain must be reached in order to attain the prescribed maximum stress. As a result, the strain range progressively increases despite the concomitant increase of the minimum strain. In conclusion, the representation of the results from the tests in load control in terms of either maximum strain or strain range is quite approximate because it only refers to their nominal values.

4. Fatigue life after a progressive deformation start-up

Since a longer aging at 100 °C should have beneficial effects on the material behavior, a further set of specimens was prepared by applying a homogenization process at 850 °C followed by an aging at 100 °C of one week instead of two hours. These specimens were then used to undergo fatigue tests which include an initial mechanical training consisting of a progressive deformation start-up, as proposed in (Casciati, *et al.* 2008, Torra, *et al.* 2009). Each fatigue test is performed as a sequence of three steps:

(a) The temperature is set at 34 °C. The machine is driven in displacement control during the loading and in load control during the unloading. This procedure enables to prevent compressions without having to assign an arbitrary lower limit to the strain as it was done in the previous tests of Table 2. Five sets of 50 loading-unloading cycles are carried out, at the rate of 0.25 Hz. Each set corresponds to a different maximum strain level: 0.8%, 1.2%, 1.5%, 2.4% and 3.2%, respectively. The time interval between two subsequent sets is 20 s. At the end of the first step, the specimen is maintained at rest for 200 seconds.

(b) The temperature is set at 21 °C. The machine is driven in displacement control during the loading and in load control during the unloading. Progressive sets of 100 loading-unloading cycles are carried out at the rate of 0.5 Hz. Each set is characterized by a different maximum strain level: 1.2%, 1.5%, 2.4%, 3.2%, 3.9%, 4.7%, and 5.5%, respectively. The strain limit selected for step c) determines the number of sets actually applied. The time interval between two subsequent sets is 70 s. At the end of this step, the specimen is maintained at rest for 200 seconds.

(c) The temperature is set at 21 °C. The machine is driven in displacement control during the loading and in load control during the unloading. Loading-unloading cycles are conducted at the rate of 0.5 Hz up to a fixed maximum strain value (equal to the one of the last sequence of cycles during the previous step), until the specimen rupture occurs.

A test with the maximum strain value of step c) equal to 5.5% was first conducted on a specimen which underwent a preliminary homogenization process of heating at 850 °C for 30 min followed by an immediate quench in water at 20°C. The result of this test is given in Fig. 7.

The same test was then repeated on a specimen whose homogenization process at 850 °C lasted 10 min (Fig. 8(a)) instead of 30 min (Fig. 7). The ragged aspect of Fig. 7 with respect to Fig. 8(a) is due to the adoption of a lower sampling frequency (4 Hz instead of 20 Hz.). Furthermore, in Fig. 7, the time interval between step a) and step b) is longer than 200 s. Nevertheless, the comparison between Fig. 7 and Fig. 8 shows that a longer homogenization process has negative consequences on the fatigue lifetime of the specimen, since only 700 cycles are performed before the specimen rupture. Therefore, all the following tests are carried out on specimens with a homogenization time of 10 min instead of 30 min.

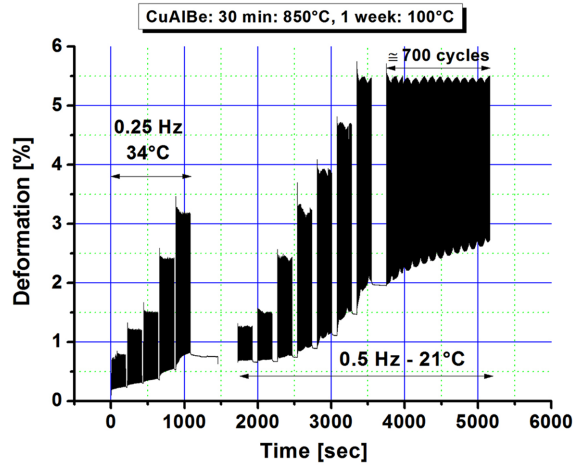


Fig. 7 CuAlBe alloy after 30 min at 850 °C and one week of aging at 100 C

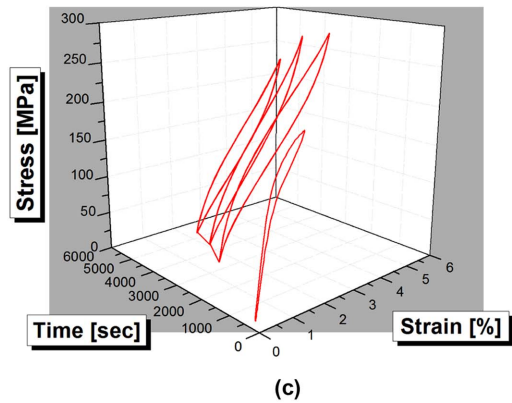
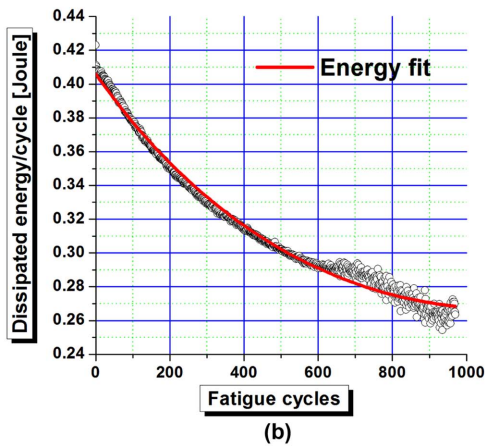
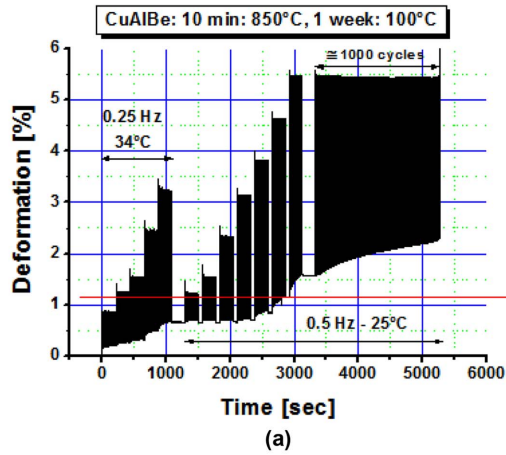


Fig. 8 CuAlBe alloy after 10 min at 850°C and one week of aging at 100 C. Maximum strain value of 5.5%. (a) Time-deformation plot; (b) energy dissipated in each cycle; (c) sketch of the loading-unloading cycles at different times of the test

In Fig. 8(a) a horizontal line marks the lower deformation limit adopted for the fatigue tests in span control described in the previous section, in order to emphasize their difference from the current tests. Fig. 8 is completed by two further plots: the energy, E , dissipated during each cycle (Fig. 8(b)) and a sketch of the loading-unloading cycles at different times during the test (Fig. 8(c)). In particular, the equation of the exponential curve fitting the data plotted in Figure.

$$E = E_0 + a [1 - \exp(-N/N_1)] + b [1 - \exp(-N/N_2)] = 0.4153 - 0.08458 [1 - \exp(-N/427.46)] - 7.37 \cdot 10^7 \{1 - \exp[N/(2.08 \cdot 10^{12})]\} \quad (1)$$

where the variable N indicates the number of cycles whose values are reported in the abscissa of Fig. 8(b).

The plot in Fig. 8(c) shows four series of three overlapping loading-unloading cycles each, which are extracted from the test results as follows. The first series is taken from the set of cycles with maximum strain of 1.5% during the initial phase of mechanical training (step a): it shows the classical hysteresis expected by a shape memory alloy in the austenite phase. The following three series refer to the beginning, the middle and the end, respectively, of the final fatigue test (step c): the deterioration of the material is evident from both the steep shape of the hysteresis loops and the progressive decrease of the maximum value of the achieved stress.

In conclusion, the following remarks arise. Up to a strain of 3-3.5% there is no evidence of creep phenomena at ambient temperature. Each set of cycles in Fig. 8(a) starts at the same deformation as the previous one, thus indicating that no residual deformation was accumulated. For higher values of maximum deformation, the residual strain due to the creep effects progressively increases during the fatigue cycles. However, the specimen can undergo 1000 successive cycles at the maximum deformation level of 5.5%.

The obtained results suggest that when the upper limit of the requested deformation is less than 5.5%, a fatigue life of more than 1000 cycles is expected. To prove the latter statement, the fatigue test is repeated for lower assignments of the maximum strain. In particular the values of 3.2% and 1.5% are selected as strain upper bounds and the results of the tests are given in Figs. 9 and 10, respectively. The fatigue life shown in Fig. 9 (2120 cycles) is more than doubled with respect to the corresponding value in Fig. 8 (1000 cycles). The increase of fatigue life is mainly associated to the low value of deformation (0.6%) recorded after the initial training in progressive deformation. This value represents the initial deformation lower limit for the following fatigue cycles. The subsequent values of minimum strain slowly increase as the material deteriorates. The deterioration process is even slower in the case of Fig. 10, where a maximum strain value of 1.5% is assigned. Nearly 40,000 cycles can be performed before the material starts deteriorating. In this case, the fatigue life is 90000 cycles.

The energy, E , dissipated during each cycle up to the strain of 3.2% is plotted in Fig. 9(b). The equation of the exponential curve fitting the data is:

$$E = E_0 + a [\exp(-N/N_1)] = 0.09563 + 0.07411 [\exp(-N/1126.46)] \quad (2)$$

where N is the number of cycles.

In Fig. 9(c), as in Fig. 8(c), four series of three loading-unloading cycles each are shown at different times during the test up to the maximum strain of 3.2%. Both the first and the second series, which refer to the initial mechanical training with 1.5% maximum strain and to the beginning of the fatigue sequence, respectively, show the classical hysteresis expected by a shape memory alloy in the austenite phase. Indeed, the maximum strain value of 3.2% assigned to perform the fatigue sequence is such that the shape of the hysteresis cycle is preserved at the beginning of the sequence. Then, the cycles of the last two series progressively assume a steeper and narrower shape which characterize the deterioration

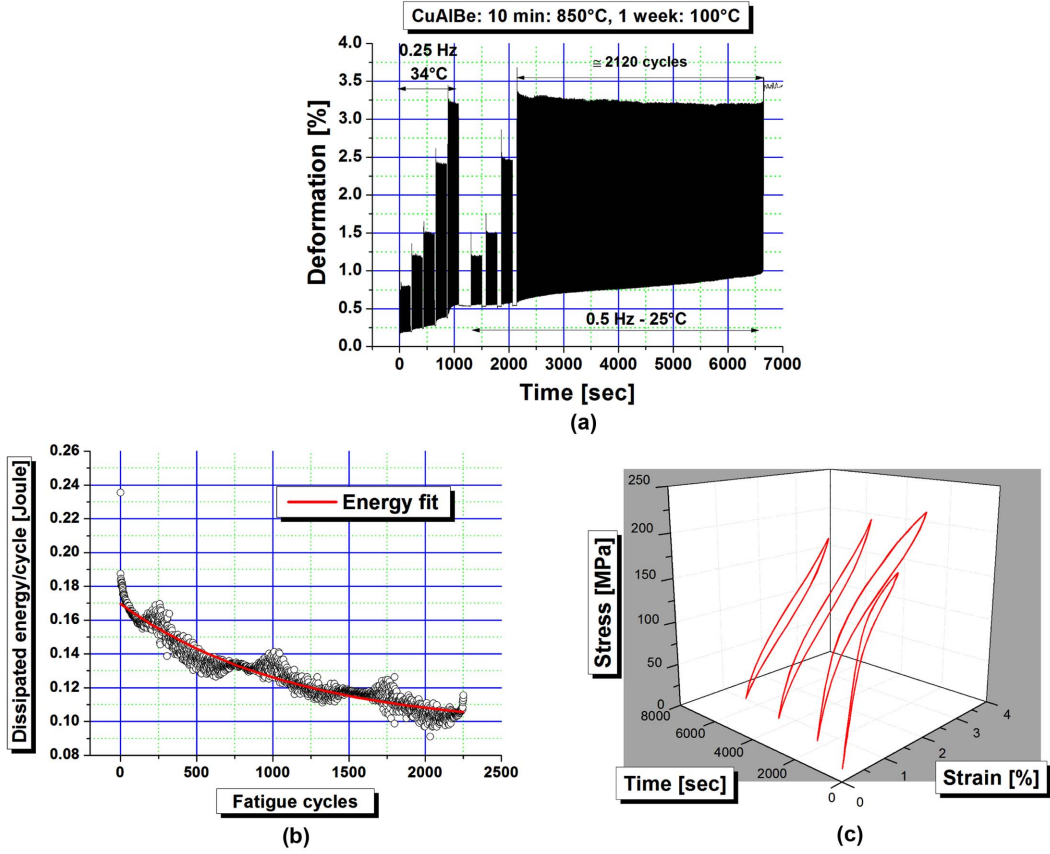


Fig. 9 CuAlBe alloy after 10 min at 850 °C and one week of aging at 100 °C. Maximum strain value of 3.2%: (a) time-deformation plot; (b) energy dissipated in each cycle; (c) sketch of the loading-unloading cycles at different times of the test

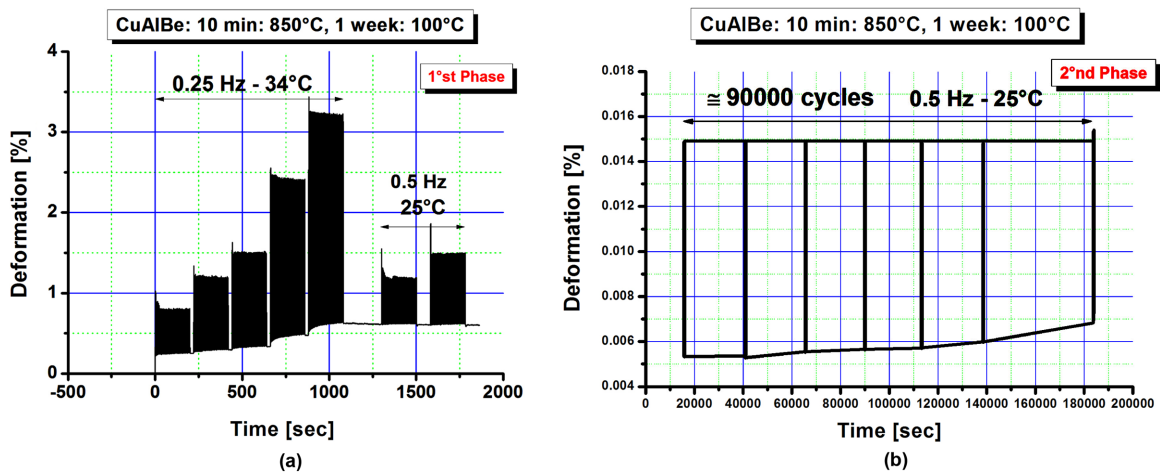


Fig. 10 CuAlBe alloy after 10 min at 850 °C and one week of aging at 100 C. Maximum strain value of 1.5%: (a) time-deformation plot for steps a and b; (b) time-deformation plot for step c

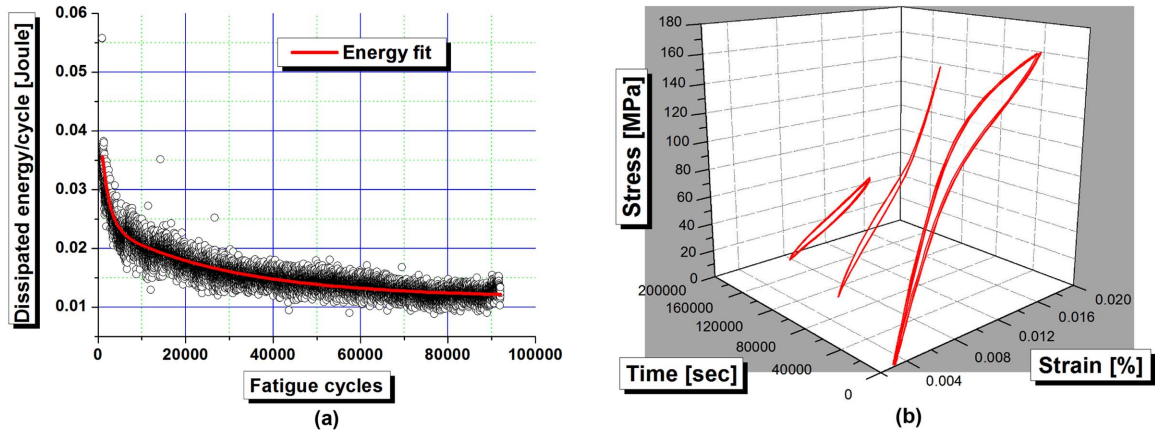


Fig. 11 CuAlBe alloy after 10 min at 850 °C and one week of aging at 100 C. Maximum strain value of 1.5%. (a) Energy dissipated in each cycle; (b) sketch of the loading-unloading cycles at different times of the test

of the material. Nevertheless, the energy per cycle shows some irregularities: it seems stabilized, when its value jumps up to starts a new regularization process.

Nevertheless, the dissipated energy per cycle shows some irregularities: it seems stabilized during the initial mechanical training, but then its value, which is given by the area of the hysteresis loop, jumps up at the beginning of the fatigue sequence, thus starting a new regularization process.

The energy, E , dissipated during each cycle up to the strain of 1.5% is plotted in Fig. 11(a). The equation of the exponential curve fitting the data in Fig. 11(a) is:

$$\begin{aligned}
 E &= E_0 + a [\exp(-N/N_1)] + b [\exp(-N/N_2)] = \\
 &= 0.01164 + 0.02039 [\exp(-N/1129)] + 0.01253 (\exp N/29989)
 \end{aligned} \quad (3)$$

where N is the number of cycles.

In Fig. 11(b), as in Figs. 8(c) and 9(c), four series of three loading-unloading cycles each are shown at different times of the test up to the maximum strain of 1.5%. In this case, the first series, which refers to the initial mechanical training with 1.5% maximum strain (step a), cannot be distinguished from the loops at the beginning of the fatigue sequence. This series shows the classical hysteresis expected by a shape memory alloy in the austenite phase. The following two series are extracted from the middle and the end of the fatigue sequence, respectively (step c): the deterioration of the material is evident from both the steep and narrow shape of the hysteresis loops and the progressive decrease of the maximum value of the achieved stress.. The dissipated energy per cycle shows the same irregularities as in Fig. 9(c), but local zooms are necessary in order to outline them.

5. Conclusions

A Ni-Ti alloy in bars of diameter 5.3 mm successfully passed most of the tests carried out in view of a standard quality control. Nevertheless, it showed unexpected viscous features related to the martensite stabilizations. Instead such a negative creep phenomenon is not observed when testing specimens of Cu-based shape memory alloy in bars of diameter 3.5 mm. The thermo-mechanical properties of such an alloy offer a temperature window which is broad enough for most civil engineering applications, and

its viscous response at constant load is negligible.

Further tests are carried out to investigate the fatigue properties of the Cu-based alloy. The main conclusions which can be drawn from the experimental results are summarized as follows:

- (1) the need of a preliminary thermo-mechanical treatment;
- (2) the dependency of the observed material behaviour on the test specifications (i.e., the assignment of either stress or strain ranges, as well as the choice of either a span or load control of the testing machine);
- (3) the strong influence of both the temperature range and the strain range.

The main result arising from the analyses of the test records is the existence of a discontinuity in the response which is dependent on the maximum strain value: below a threshold value of strain (3%) the fatigue life is quite satisfactory; above it, the fatigue life reduces drastically to a few hundreds of cycles.

Acknowledgments

This study is supported by grants from the Athenaeum Research Fund of the University of Catania (PRA07).

References

- Auricchio, F., Faravelli, L., Magonette, G. and Torra, V. (2001), *Shape memory alloys: advanced in modelling and applications*, CIMNE, Barcelona, Spain.
- Casciati, F. and Faravelli, L. (2004), "Experimental characterization of a cu-based shape memory alloy toward its exploitation in passive control devices", *J. Phys. IV*, **115**, 299-306.
- Casciati, F. and Faravelli, L. (2009), "A passive control device with SMA components: from the prototype to the model", *Struct. Control Health Monit.*, DOI: 10.1002/stc.328.
- Casciati, F. and van der Eijk, C. (2008), "Variability in mechanical properties and microstructure characterization of CuAlBe shape memory alloys for vibration mitigation", *Smart Struct. Syst.*, **4**(2), 103-122.
- Casciati, F., Casciati, S. and Faravelli, L. (2007), "Fatigue characterization of a cu-based shape memory alloy", *Proc. of the Estonian Academy of Sciences*, **56**, 207-217.
- Casciati, F., Faravelli, L. and Hamdaoui, K. (2007), "Shape memory alloy bars assembled in a base isolator", *Proc. of the ANCCER Conf.*, Hong Kong.
- Casciati, F., Faravelli, L., Isalgue, A., Martorell, F., Soul, H. and Torra, V. (2008), "SMA fatigue in civil engineering applications", *Adv. Sci. Technol.*, Trans Tech Publications, Switzerland, **59**, 168-177.
- Casciati, S. and Faravelli, L. (2004), "Thermo-mechanic characterization of a cu-based shape memory alloy", *Proc. of Int. Symposium on Network and Center-Based Research for Smart Structures Technologies and Earthquake Engineering*, July 6-9, Osaka Univ., Suita, Osaka, Japan, 377-388.
- Casciati, S. and Faravelli, L. (2006), "Fatigue tests of a cu-based shape memory alloy", *Proc. of the 4th World Conf. on Structural Control & Monitoring*, San Diego, USA.
- Casciati, S. and Faravelli, L. (2008), "Structural components in shape memory alloy for localized energy dissipation", *Comput. Struct.*, **86**, 330-339.
- Casciati, S. and Hamdaoui, K. (2008), "Experimental and numerical studies toward the implementation of shape memory alloy ties in masonry structures", *Smart Struct. Syst.*, **4**(2), 153-170.
- Casciati, S. and Marzi, A. (2008), "Comparison of the thermo-mechanical behaviour of different shape memory alloys", *Proc. of the 4th European Conf. on Structural Control*, St. Petersburg, Russia, **1**, 141-148.
- Casciati, S. and Osman, A. (2005), "Damage assessment and retrofit study for the Luxor Memnon Colossi", *Struct. Control Health Monit.*, **12**, 139-156.
- Montecinos, S., Moroni, M.O. and Sepúlveda, A. (2006), "Superelastic behaviour and damping capacity of CuAlBe

- alloys”, *Mater. Sci. Eng. A*, **419**, 91-97.
- Olsen, J.S., van der Eijk, C. and Zhang, Z.L. (2008), “Analysis of shape memory alloy based seismic damper”, *Smart Struct. Syst.*, **4**(2), 137-152.
- Otsuka, K. and Wayman, C.M. (1999), *Shape memory materials*, Cambridge University Press.
- Torra, V., Isalgue, A., Auguet, C., Carreras, G., Lovey, F.C., Soul, H. and Terriault, P. (2009), “Damping in civil engineering using SMA. the fatigue behavior and stability of CuAlBe and NiTi alloys”, *J. Mater. Eng. Perform.*, DOI: 10.1007/s11665-009-9442-6, May.
- Torra, V., Isalgue, A., Martorell, F., Casciati, F., Lovey, F.C., Peigney, M., Terriault, P., Tirelli, D. and Zapico, B. (2009), “SMA in mitigation of extreme loads in civil engineering: damping of earthquake effects in family houses and in wind/rain perturbations on stayed cables in bridges”, *Proc. PROTECT*, Japan.
- Torra, V., Isalgue, A., Martorell, F., Terriault, P. and Lovey, F.C. (2007), “Built in dampers for family homes via SMA: An ANSYS computation scheme based on mesoscopic and microscopic experimental analyses”, *Eng. Struct.*, **29**, 1889-1902.

FC